Review of "Look-up tables resolved by complex refractive index to correct particle sizes measured by common research-grade optical particle counters" by Formenti et al.

Steven Howell

January 20, 2022

I like the fundamental idea behind the paper; an easy to use, authoritative compilation of the relationships between particle size, refractive index, and instrument response for common OPCs would be a valuable contribution to the literature. Unfortunately, this manuscript contains some major errors that must be corrected before it can be published. Much of the difficulty appears to stem from misunderstanding (or mis-describing) the optical geometry of the UHSAS and Grimm OPCs. The discussion appears not to recognize that they collect light asymmetrically around the polarized laser beam, which renders the fundamental equation incorrect.

It will take significant recalculation, but I do think the concept behind the paper is sufficiently valuable that a resubmission after corrections would be welcome.

Major issues

Scattering from polarized light

Here is a somewhat simplified version of Eq. 1 in the manuscript:

$$C_{\text{sca}} = \frac{\pi}{k^2} \int_0^{2\pi} \int_{\theta_{\min}}^{\theta_{\max}} \left(|S1|^2 + |S2|^2 \right) \sin\theta \; w_{\text{optics}}(\theta, \phi) \; d\theta \; d\phi \tag{1}$$

In this equation the scattered intensity $|S1|^2 + |S2|^2 = I_s$ is integrated over the angles θ and ϕ sensed by the OPC optics.

However, that intensity is correct only for unpolarized light. If the illumination is polarized, I_s becomes a function of ϕ (as well as θ, D_p, k, and m). Bohren and Huffman (1983) discuss scattering from a sphere:

> From Bohren and Huffman (1983) section 4.4.4
>
> The relation between the incident and scattered Stokes parameters follows from

(4.75):

$$\begin{pmatrix} I_s \\ Q_s \\ U_s \\ V_s \end{pmatrix} = \frac{1}{k^2 r^2} \begin{pmatrix} S_{11} & S_{12} & 0 & 0 \\ S_{12} & S_{11} & 0 & 0 \\ 0 & 0 & S_{33} & S_{34} \\ 0 & 0 & -S_{34} & S_{33} \end{pmatrix} \begin{pmatrix} I_i \\ Q_i \\ U_i \\ V_i \end{pmatrix},$$
$$S_{11} = \frac{1}{2}(|S_2|^2 + |S_1|^2), \qquad S_{12} = \frac{1}{2}(|S_2|^2 - |S_1|^2), \tag{2}$$
$$S_{33} = \frac{1}{2}(S_2^* S_1 + S_2 S_1^*), \qquad S_{34} = \frac{i}{2}(S_1 S_2^* - S_2 S_1^*).$$

Only three of these four matrix elements are independent: $S_{11}^2 = S_{12}^2 + S_{33}^2 + S_{34}^2$.

If the incident light is 100% polarized *parallel* to a particular scattering plane (it makes no difference which scattering plane), the Stokes parameters of the scattered light are

$$I_s = (S_{11} + S_{12})I_i, \quad Q_s = I_s, \quad U_s = V_s = 0, \tag{3}$$

where we have omitted the factor $1/k^2r^2$. Thus, the scattered light is also 100% polarized parallel to the scattering plane. We denote by $i_\parallel$ the scattered irradiance per unit incidence irradiance given that the incident light is polarized parallel to the scattering plane:

$$i_\parallel = S_{11} + S_{12} = |S_2|^2. \tag{4}$$

If the incident light is polarized *perpendicular* to the scattering plane, the Stokes parameters of the scattered light are

$$I_s = (S_{11} - S_{12})I_i, \quad Q_s = -I_s, \quad U_s = V_s = 0, \tag{5}$$

Thus, the scattered light is also polarized perpendicular to the scattering plane. We denote by $i_\perp$ the scattered irradiance per unit incident irradiance given that the incident light is polarized perpendicular to the scattering plane:

$$i_\perp = S_{11} - S_{12} = |S_1|^2. \tag{6}$$

If the incident light is *unpolarized*, the Stokes parameters of the scattered light are

$$I_s = S_{11} I_i, \quad Q_s = S_{12} I_s, \quad U_s = V_s = 0. \tag{7}$$

Eq. 3 and Eq. 5 indicate that as the angle ϕ changes from parallel to perpendicular to the laser polarization, I_s changes from

$$I_{s,\parallel} = (S_{11} + S_{12})I_i = |S_2|^2 \quad \text{to} \tag{8}$$
$$I_{s,\perp} = (S_{11} - S_{12})I_i = |S_1|^2. \tag{9}$$

I expect that $S1$ and $S2$ in the manuscript are the amplitude scattering matrix

elements S_1 and S_2 from the second line of Eq. 2, so Eq. 1 in the manuscript is essentially using $I_s = S_{11} I_i = |S_2|^2 + |S_1|^2$ from Eq. 7. That is correct only for an unpolarized light source. It happens to work for instruments that gather light symmetrically around the beam, and thus average $|S_1|^2$ and $|S_2|^2$. That is essentially true for the PCASP (ignoring the holes in the mirror for the particle beam) and the CDP, but is not the case for the UHSAS or the Grimm.

The simplest way to get the I_s as a function of ϕ, the angle between the polarization plane of the laser and of the scattered light is to modify Eq. 1 to

$$C_{\text{sca}} = \frac{\pi}{k^2} \int_0^{2\pi} \int_{\theta_{\text{min}}}^{\theta_{\text{max}}} \left(|S_1|^2 \sin^2 \phi + |S_2|^2 \cos^2 \phi \right) \sin\theta \; w_{\text{optics}}(\theta, \phi) \; d\theta \; d\phi \qquad (10)$$

but beware that it could be $\left(|S_2|^2 \sin^2 \phi + |S_1|^2 \cos^2 \phi \right)$, depending on how the amplitude scattering matrix is defined in your software. It is enlightening to play around with rotating Stokes parameters using transformation matrices.

UHSAS geometry

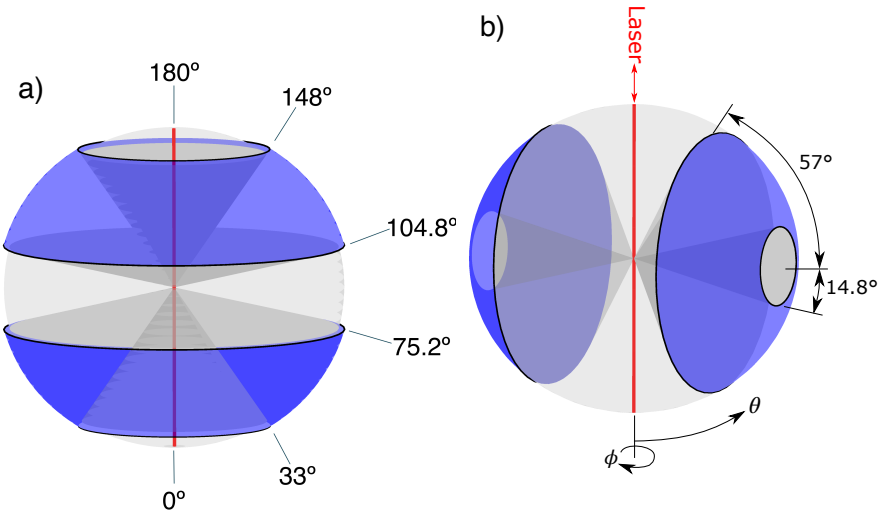

Figure 1: Left: UHSAS scattering angles as the manuscript seems to describe them. Right: the actual angles sensed by the UHSAS, taken from Howell et al. (2021).

I found the description of the scattering angles detected by the UHSAS to be confusing, and possibly in error. To be fair, the descriptions of the scattering angles in the sources used in the manuscript (Brock et al. 2016; Cai et al. 2008; Petzold et al. 2013) are not entirely clear. Even the manual (Droplet Measurement Technologies 2017) has language easy to misinterpret, though the geometry is illustrated clearly.

The optics used in the modeling of the UHSAS are mentioned in Section 2.1

Lines 188–190

the optically active range is circularly symmetric from 33° to 148°, with a blind region between 75.2 and 104.8°

and in Table 1

Angular Range of scattered light
33°–75.2° + 104.8°–148°

Reading those, it appears that the Mie calculations were for the geometry shown in Fig. 1a, but the actual geometry is shown in Fig. 1b. It is entirely possible that the authors understood the UHSAS configuration and attempted to model it with their Mie calculations (with an inaccurate equation; see above) but retained the confusing language from earlier papers. Ironically, if the UHSAS had the configuration shown in Fig. 1, Eq. 1 in the manuscript would be correct.

Grimm geometry

So far, I have failed to find a sufficiently detailed description of the optics of the Grimm to be confident of how to model it for Mie calculations, but as with the UHSAS, the description of the Grimm geometry in the manuscript does not agree with illustrations in the literature. Again, it is quite possible that the modeled geometry is correct, but that the description is a bit sloppy.

Ferrero et al. (2011) and Heim et al. (2008) have similar descriptions descriptions of the Grimm, mentioning a 120° or 121° parabolic mirror centered at 90° from the illuminating laser and from the particle beam. The mirror reflects light to a photodetector directly opposite the mirror. That photodetector also receives scattered light directly from the particles in a circular region 18° across. I have found no documentation of the polarization of the laser with respect to the the detector. Grimm and Eatough (2009) is confusing and seems to indicate that the mirror only spans a region of $\theta = 30°$ around 90°.

The description in the manuscript does not seem to agree with any of the three references:

Lines 203–207

These particle counters operate at 655 nm, and measure light scattered by the direct beam from 30° to 150° and by the reflected beam between 81° and 98° due to two face-to-face parabolic mirrors (opening angles of 120° and 18°, respectively) that collect light around a mean scattering angle of 90° (Heim et al., 2008). Like the PCASP, the light scattered between 81° and 98° has twice the weight relative to the intensity within 30°–81° and 98°–150°.

Heim et al. (2008) do not mention two mirrors, and the small angle range 81°–98° is the direct beam to the photosensor, not a reflection. My guess of the scattering angles detected by the Grimm OPC based on Ferrero et al. (2011) and Heim et al. (2008) is shown in Fig. 2. Reading your description, all scattered light with scattering angle θ between 30° and 150° is detected, with that between 81° and 98° doubled. Actually, for $\theta = 90$, only light with ϕ from 30° to 150° and from 261° to 279° will be detected. At $\theta = 45°$ or 135°, only ϕ from approximately 50° to 130° will be included.

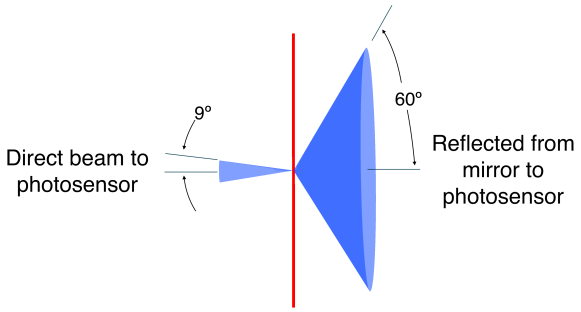

Figure 2: Scattering angles detected by the Grimm OPC

Supplement Table 1 and Fig. 5

Ultimately, it really doesn't matter very much for the substance of the paper, but there are a whole cascade of problems here that really ought to be corrected.

- Figure 5 has unacceptably poor resolution. The exponents on the tick labels are completely illegible and all of the axis labels are hard to read.
- In Table S1, the second "Mode 2" should presumably be "Mode 3".
- In Table S1, the median diameters are off by a factor of 1000 in modes 1 and 2 or in mode 3. I don't have the second edition of Seinfeld and Pandis, but looking at both the first and third editions, there is a table giving three mode parameters for ambient aerosol types including dust:

Desert	N (cm^3)	D_p (µm)	$\log \sigma$
Mode I	726	0.002	0.247
Mode II	114	0.038	0.770
Mode III	0.178	21.6	0.438

  So it appears that you either misread Seinfeld and Pandis or just neglected to note that Mode 1 and 2 diameters are in nm rather than µm.

- There is actually an error in the Seinfeld and Pandis table! Looking at their source, Jaenicke (1993), N_{tot} for Mode 1 is actually 1140.

- I think the solid line in the right-hand plot of Fig. 5 ought to be what I get from plotting Eq. 2 in the supplement using the parameters in Table S1. I have not been able to figure out what is being plotted. Rather than modes at 2 µm, 37 µm and 21.6 µm (or 0.002 µm, 0.037 µm and 21.6 µm) the modes plotted are at 0.048 µm and 0.28 µm.

Since the point of Fig 5 is to illustrate the artifacts caused by the CDP, it doesn't matter much whether the base distribution accurately reflects previous literature or real distributions, so your example is still valid, but please be more careful describing it.

Minor issues

Bad links This will probably be corrected by the copy editors, but it is annoying that none of the links containing hyphens work. Most work if I edit the URLs and substitute hyphens for whatever is in there that looks a lot like a hyphen.

Particle heating in the UHSAS: The UHSAS has a far more powerful laser than the other OPCs considered, with a circulating power of about 1 kW. That is necessary to obtain detectable scattering from 60 nm particles given the long wavelength used to suppress Mie wiggles. The upshot is that particles that absorb in the near IR will heat, potentially enough to evaporate much of their mass away and appear much smaller (Howell et al. 2021; Yokelson et al. 2011). It is probably not practical to add another column to your data files with estimated heating, since that is a function of pressure and the poorly known efficiency with which thermal energy is transferred to air molecules as they collide with the heated particles. So the best that can be done is to warn readers that the UHSAS will undersize absorbing particles.

OPC wavelength and refractive index The UHSAS uses an IR wavelength of 1054 nm while the other OPCs considered are in the range of 632 nm to 655 nm, which are in the visible range. It should be mentioned in the paper that refractive index is a function of wavelength and one needs to pay attention to that.

Equation formatting I'm sure the copy editors will correct it all, but the use of italics and roman fonts in the equations bears no resemblance to the Copernicus mathematics formatting rules.

Figure labels As a minor nit, you use "um" rather than "µm". Most graphics languages, including IDL, are capable of producing Greek letters.

Line 186 and Figure 2, UHSAS: The UHSAS size bins can be arbitrarily configured, but are typically equally spaced on a log scale ($d \log D_p$ is constant). That is not what is illustrated in Fig. 2, which appears to show bins equally spaced on a linear scale. In addition, while there may be some instances where UHSAS size bins start at 0.04 µm, all of the UHSAS datasets I've seen start at 0.06 µm.

Line 218 (Eq. 1): The use of *CRI* is clumsy within equations. The usual standard is to call it m and it would be perfectly reasonable to use it in this paper. There is possible confusion since it is usually defined as $m = n + ik$, where n is the real part of the refractive index and k, the imaginary part of the refractive index could be confused with the wavenumber k, but there are at least three ways around that problem. Bohren and Huffman (1983) use roman k for wavenumber and italic k for imaginary refractive index. Mishchenko, Travis, and Lacis (2006) use $m = m_{\mathrm{R}} + im_{\mathrm{I}}$. One can also use wavelength λ instead of wavenumber in Eq. 1. I notice that you do use k to refer to the refractive index when describing the dataset in lines 274–275 and 282–283. Yes, this is a very small nit.

Line 267: You should specify that you are indeed using log base 10. Yes, the usual standard is to use 'ln" for log base e and "log" for base 10, but mentioning it could avoid confusion.

Lines 282–297 The second and third file types are not useful for the UHSAS, since the size bins are not correct (at least for the UHSAS datasets I've seen). Of course, it is straightforward to recalculate them from the intensity files.

Line 460: The reference to the IDL routine `http://www.atm.ox.ac.uk/code/mie/mie_single.html` does not work, yielding error 404. It appears that it has changed to `http://eodg.atm.ox.ac.uk/MIE/mie_single.html`

Table 1: The refractive index of PSL drops as wavelength increases (Ma et al. 2003; Nikolov and Ivanov 2000; Velazco-Roa and Thennadil 2007). At 1054 nm, the wavelength of the UHSAS, $m_{\mathrm{PSL}} \approx 1.572 + 0.001i$.

Supplement equations: Equation 2 precedes Eq. 1, which is followed by another, different Eq. 2.

Supplement Fig. 1 This set of figures is inadequately explained. What are the white and black lines in the colorbars at ~ 1.2 and ~ 1.7? Presumably the imaginary part of the refractive index k was held constant for the panels showing the effects of changing the real part. What was that k? Similarly, what was the real part of the refractive index n in the panels on the right where you were exploring k?

Supplement Fig. 1 Much of the regular structure in the left panels is almost certainly an artifact. It is exceedingly unlikely that there would be a regular pattern at increments of 0.01 in n regardless of the OPC wavelength and optical configuration.

References

Bohren, C. F. and D. R. Huffman (1983). *Absorption and Scattering of Light by Small Particles*. New York: Wiley, xiv, 530 p.

Brock, C. A., N. L. Wagner, B. E. Anderson, A. Beyersdorf, P. Campuzano-Jost, D. A. Day, G. S. Diskin, T. D. Gordon, J. L. Jimenez, D. A. Lack, J. Liao, M. Z. Markovic, A. M. Middlebrook, A. E. Perring, M. S. Richardson, J. P. Schwarz, A. Welti, L. D. Ziemba, and D. M. Murphy (2016). "Aerosol optical properties in the southeastern United States in summer – Part 2: Sensitivity of aerosol optical depth to relative humidity and aerosol parameters". *Atmospheric Chemistry and Physics* 16.8, pp. 5009–5019. DOI: 10.5194/acp-16-5009-2016.

Cai, Y., D. C. Montague, W. Mooiweer-Bryan, and T. Deshler (Sept. 2008). "Performance characteristics of the ultra high sensitivity aerosol spectrometer for particles between 55 and 800nm: Laboratory and field studies". *Journal of Aerosol Science* 39.9, pp. 759–769. DOI: 10.1016/j.jaerosci.2008.04.007.

Droplet Measurement Technologies (2017). *Operator Manual: Ultra High Sensitivity Aerosol Spectrometer (UHSAS)*. Boulder, CO USA.

Ferrero, L., G. Mocnik, B. Ferrini, M. Perrone, G. Sangiorgi, and E. Bolzacchini (2011). "Vertical profiles of aerosol absorption coefficient from micro-Aethalometer data and Mie calculation over Milan". *Science of The Total Environment* 409.14, pp. 2824–2837. DOI: https://doi.org/10.1016/j.scitotenv.2011.04.022.

Grimm, H. and D. J. Eatough (2009). "Aerosol Measurement: The Use of Optical Light Scattering for the Determination of Particulate Size Distribution, and Particulate Mass, Including the Semi-Volatile Fraction". *Journal of the Air & Waste Management Association* 59.1, pp. 101–107. DOI: 10.3155/1047-3289.59.1.101.

Heim, M., B. J. Mullins, H. Umhauer, and G. Kasper (2008). "Performance evaluation of three optical particle counters with an efficient "multimodal" calibration method". *Journal of Aerosol Science* 39.12, pp. 1019–1031. DOI: doi.org/10.1016/j.jaerosci.2008.07.006.

Howell, S. G., S. Freitag, A. Dobracki, N. Smirnow, and A. J. Sedlacek III (2021). "Undersizing of aged African biomass burning aerosol by an ultra-high-sensitivity aerosol spectrometer". *Atmospheric Measurement Techniques* 14.11, pp. 7381–7404. DOI: 10.5194/amt-14-7381-2021.

Jaenicke, R. (1993). "Tropospheric Aerosols". eng. In: *Aerosol-Cloud-Climate Interactions*. Ed. by P. V. Hobbs. International Geophysics Series (V. 54). Oxford: Elsevier Science & Technology.

Ma, X., J. Q. Lu, R. S. Brock, K. M. Jacobs, P. Yang, and X.-H. Hu (Dec. 2003). "Determination of complex refractive index of polystyrene microspheres from 370 to 1610 nm". *Physics in Medicine and Biology* 48.24, pp. 4165–4172. DOI: 10.1088/0031-9155/48/24/013.

Mishchenko, M. I., L. D. Travis, and A. A. Lacis (2006). *Scattering, Absorption, and Emission of Light by Small Particles*. 3rd electronic. New York: NASA Goddard Institute for Space Studies.

Nikolov, I. D. and C. D. Ivanov (May 2000). "Optical plastic refractive measurements in the visible and the near-infrared regions". *Appl. Opt.* 39.13, pp. 2067–2070. DOI: 10.1364/AO.39.002067.

Petzold, A., P. Formenti, D. Baumgardner, U. Bundke, H. Coe, J. Curtius, P. J. DeMott, R. C. Flagan, M. Fiebig, J. G. Hudson, J. McQuaid, A. Minikin, G. C. Roberts, and J. Wang (2013). "In Situ Measurements of Aerosol Particles". eng. In: *Airborne Measurements for Environmental Research*. Weinheim, Germany: Wiley-VCH Verlag GmbH & Co. KGaA, pp. 157–223.

Velazco-Roa, M. A. and S. N. Thennadil (June 2007). "Estimation of complex refractive index of polydisperse particulate systems from multiple-scattered ultraviolet-visible-near-infrared measurements". *Appl. Opt.* 46.18, pp. 3730–3735. DOI: 10.1364/AO.46.003730.

Yokelson, R. J., I. R. Burling, S. P. Urbanski, E. L. Atlas, K. Adachi, P. R. Buseck, C. Wiedinmyer, S. K. Akagi, D. W. Toohey, and C. E. Wold (2011). "Trace gas and particle emissions from open biomass burning in Mexico". *Atmospheric Chemistry and Physics* 11.14, pp. 6787–6808. DOI: 10.5194/acp-11-6787-2011.